Title

Ozone-induced climate change propped up by the Southern Hemisphere oceanic front

Authors

Fumiaki Ogawa, Geophysical Institute, University of Bergen, Bergen, Norway, and Bjerknes Centre for Climate Research, Bergen, Norway.

Nour-Eddine Omrani, Geophysical Institute, University of Bergen, Bergen, Norway, Bjerknes Centre for Climate Research, Bergen, Norway, and Helmholtz Centre for Ocean Research Kiel (GEOMAR), Kiel, Germany.

Kazuaki Nishii, Research Center for Advanced Science and Technology, University of Tokyo, Tokyo, Japan.

Hisashi Nakamura, Research Center for Advanced Science and Technology, University of Tokyo, Tokyo, Japan, and Japan Agency for Marine-Earth Science and Technology, Yokohama, Japan

Noel Keenlyside, Geophysical Institute, University of Bergen, Bergen, Norway, and Bjerknes Centre for Climate Research, Bergen, Norway.

Corresponding author: F. Ogawa, Geophysical Institute, University of Bergen, Bergen, Norway. Allégaten 70, Bergen, 5007, Norway. (fumiaki.ogawa@gfi.uib.no)

Key points

- Oceanic fronts can affect the ozone-induced surface climate change
- Oceanic fronts can enhance the stratosphere and troposphere dynamical coupling
- A realistic westerly trend requires a realistic oceanic front in a climate model

Abstract

The late 20th century was marked by a significant summertime trend in the Southern Annular Mode (SAM), the dominant mode of tropospheric variability in the extratropical Southern Hemisphere (SH). This trend with poleward-shifting tropospheric westerlies was attributed to downward propagation of stratospheric changes induced by ozone depletion. However, the role of the ocean in setting the SAM response to ozone depletion and its dynamical forcing remains unclear. Here we show, using idealized experiments with a state-of-the-art atmospheric model and analysis of IPCC climate simulations, that frontal sea-surface temperature gradients in the midlatitude SH are critical for translating the ozone-induced stratospheric changes down to the surface. This happens through excitation of wave forcing, which controls the vertical connection of the tropospheric SAM with the stratosphere, and shows the importance of internal tropospheric dynamics for stratosphere/troposphere coupling. Thus, improved simulation of oceanic fronts may reduce uncertainties in simulating SH ozone-induced climate changes.

Index terms and key words

Index terms: 3305, 3319, 3337, 3339, 3362

Key words: ozone-induced climate change, ozone depletion, troposphere-stratosphere coupling, southern annular mode, mid-latitude westerly, oceanic front

1. Introduction

Recent observations indicate that in the late 20th century the tropospheric westerly jet axis in the Southern Hemisphere (SH) shifted poleward (Figure 1a) [*Thompson and Solomon,* 2002; *Marshall*, 2003] leading to positive trend in the Southern Annular Mode (SAM) [*Thompson and Wallace*, 2000; *Lorenz and Hartmann*, 2001; *Thompson et al.*, 2011]. This trend was reflected in strengthening of the surface westerlies on the poleward side (~60°S) of their climatological axis (~50°S) and weakening on the equatorward side (~35°S) (Figure 1a). While the observed SAM-trend in most of the seasons has been attributed, at least in part, to the anthropogenic increase in greenhouse gases [*Shindell and Schmidt*, 2004; *Cai and Cowan*, 2007], the summertime trend has been shown to be driven mainly by the depletion of stratospheric ozone (the "ozone hole") over Antarctica [*Thompson and Solomon*, 2002; *Thompson et al.*, 2011; *Gillett and Thompson*, 2003; *Polvani et al.*, 2011]. The ozone hole induces strengthening of the polar vortex in the Antarctic stratosphere, which is then transmitted into the troposphere as the positive SAM trend by austral summer [*Thompson and Solomon*, 2002; *Thompson et al.*, 2011; *Gillett and Thompson*, 2003]. While several possible mechanisms for controlling the transmission of the high-latitude stratospheric signal into the troposphere have been proposed [*Thompson et al.,* 2011; *Yang et al.,* 2015], it has been pointed out that the downward influence through the SAM requires feedback forcing from tropospheric synoptic-scale eddies [*Yang et al.*, 2015].

Recent studies have indicated that a sharp gradient in midlatitude SST (oceanic front) maintains the cross-frontal gradient of near-surface air temperature (i.e., baroclinicity) [*Nakamura et al.*, 2008; *Nakamura et al.*, 2004; *Hotta and Nakamura*, 2011; *Nonaka et al.*, 2009], which acts to strengthen both migratory eddies and the eddy-driven westerly polar front jet (PFJ) climatologically [*Nakamura et al.*, 2008; *Ogawa et al.*, 2012]. Oceanic fronts in the summertime SH are nearly circumpolar around 45°S (Figure 1b), maintained by the confluence of warm subtropical currents with the cool Antarctic Circumpolar Current (ACC). The behavior of the SAM, manifested as the most dominant temporal fluctuations of the PFJ axis, has been shown to be sensitive to the oceanic front intensity [*Nakamura et al.*, 2008; *Sampe et al.*, 2013]. It is therefore important to ask how significant this oceanic front is for the downward influence of the ozone hole on the late 20th-century SAM trend and associated changes in the surface climate. To address this issue we performed four idealized experiments with an atmospheric general circulation model (AGCM) driven by combinations of two different SST profiles and two different ozone concentration distributions.

2. Experimental Design

We used the Hamburg version of the European Centre AGCM, ECHAM5 [*Roeckner et al.*, 2003]. Its horizontal resolution is T63 (equivalent to ~180km grid intervals), which is not particularly high but still sufficient for resolving SST gradients across the SH oceanic frontal zones. The model has 39 vertical levels up to 0.01hPa. The lower boundary of the AGCM is set as the fully global ocean without any landmass, and the SST fields prescribed are zonally symmetric and varying seasonally. This idealized "aqua-planet" setting eliminates planetary-scale stationary waves forced by topography and land-sea thermal contrasts, to mimic the SH conditions. The meridional SST profiles given to the model are based on the climatological-mean (1982-2007) monthly OISST data provided by NOAA [*Reynolds et al.*, 2007]. One of the two SST profiles is taken from the South Indian Ocean at 60°E. It is characterized by a steep SST gradient observed across a prominent oceanic front at 45°S throughout the year (black lines in Figures 2a-b and S1a), where the warm Agulhas Return Current is confluent with the cool ACC (Figure 1b). In the other SST profile, the particular frontal gradient has been eliminated (green lines in Figures 2a-b and S1b; see the supporting information for details) by warming the subpolar ocean artificially.

The zonally averaged ozone profiles that are given to the AGCM are taken from the JRA-25 reanalysis data [*Onogi et al.*, 2007] for the following two 3-year periods. One is from 1979 to 1981 that corresponds to the beginning of the ozone depletion, and the other from 1999 to 2001 when the ozone concentration reaches its minimum. The two prescribed stratospheric ozone profiles differ by nearly 50% over the polar region in September and October (Figure 2c), which is consistent with the observed depletion, though somewhat underestimated.

Each of the four AGCM experiments as combinations of two different SST and ozone profiles was conducted for 49 years, after a 3-year spin-up. Responses in the atmospheric circulation to the ozone depletion are defined as the differences in the respective 49-year averages for pairs of experiments with and without the ozone depletion under the same SST profiles. Owing to the aforementioned zonal symmetries in the SST and ozone profiles imposed onto the model, the responses exhibit a high degree of zonal symmetry and we therefore discuss zonally averaged statistics throughout this paper.

3. Simulated tropospheric response to the ozone depletion

Figures 3a and 3b show time-height sections of the zonal-mean westerly response in midlatitudes (45~60°S) to the stratospheric ozone depletion with and without the oceanic front, respectively. For simplicity, the stratosphere and troposphere are referred to as layers in which air pressure is lower and higher than 200hPa, respectively. Regardless of the presence of the oceanic front, the ozone depletion results in the intensification of the stratospheric westerlies in spring through summer as observed. In contrast, a tropospheric response in late November through mid-December is found only in the presence of the oceanic front (Figure 3a), and the response is consistent with the observed trend in geopotential height (Figure 1b of ref. 1). This midlatitude tropospheric westerly response in early summer (Figures 3a and S3a) corresponds well to the observed positive SAM trend, which is manifested in the troposphere as the westerly acceleration poleward of the climatological PFJ axis [*Limpasuvan and Hartmann, 2000*] (blue dashed line in Figures S2a and S3a).

The westerly response is consistent with enhanced westerly acceleration driven by eddy forcing, as estimated from the divergence of the Eliassen-Palm flux [*Andrews et al.*, 1987]. In the following, the eddy component defined as daily-mean local deviations of a given variable from its zonal mean is decomposed into two sub-components: synoptic and planetary-scale waves with zonal wavenumbers greater than 3 and less than 4, respectively. The ozone-induced strengthening of the stratospheric polar vortex is reinforced mainly by the planetary-scale waves (Figures S4 and S5), which occurs regardless of the oceanic front but is stronger when it is present. This result is consistent with the enhanced intensification of the stratospheric westerlies in November in the presence of oceanic front (Figures 3a-b). The tropospheric westerly acceleration then occurs as the positive SAM response only in the presence of SST front (Figures 3a-b), which is contributed by both the planetary and synoptic-scale waves (Figures S3c and

S4c-d). The positive SAM response is then maintained mainly through feedback forcing by the synoptic-scale waves (Figures S4b, e-f). The importance of the planetary (synoptic) scale waves in the stratosphere (troposphere) simulated in the presence of oceanic front is consistent with the findings by *Yang et al.* [2015].

The oceanic front activates not only the synoptic-scale waves (Figure S3f) through strengthening and maintaining the surface baroclinicity but also the planetary-scale waves (Figure S3e) presumably through non-linear interactions among the synoptic-scale waves [*Scinocca and Hanes,* 1998]. In the experiments without the oceanic front, in contrast, neither the activity of tropospheric eddies nor their westerly acceleration exhibit coherent significant changes in responding to the ozone depletion (Figures S3d and S5); this is consistent with no significant westerly response in the troposphere (Figure S3b). This suggests that activation of tropospheric eddies by near-surface baroclinicity associated with the midlatitude oceanic front (Figures S2d-e) can be crucial for the observed transmission of the ozone-induced westerly trend from the stratosphere into the troposphere.

4. Vertical coupling of the SAM as internal variability

The oceanic front is important not only for the ozone-induced climatic trend but also for year-to-year internal variability of the tropospheric SAM in summer. The observed connection between stratospheric year-to-year variability and the tropospheric SAM is pronounced from late spring to early summer [*Thompson and Wallace*, 2000; *Thompson et al.*, 2005]. We focus on the leading mode of the year-to-year variability of the stratospheric polar vortex on 15th November, the day when the stratospheric westerly response to the ozone depletion is most significant

(Figure 3a). The leading mode has been identified through an empirical orthogonal function (EOF) analysis applied to zonal-mean year-to-year anomalies of 13-hPa westerlies between 90°S and 20°S after exposed to 31-day running mean (See supporting information for details). Time-height sections of midlatitude zonal-mean westerly anomalies associated with the dominant year-to-year variability of the stratospheric polar vortex are shown in Figures 3c-d. Significant tropospheric westerly anomalies from late spring to midsummer are reproduced only in the experiments with the oceanic front. Although its duration is slightly longer, the tropospheric signal (Figure 3c) shows good correspondence with the one associated with the ozone-induced tropospheric climate trend (Figure 3a). In fact, in the presence of the oceanic front, the meridional structure of the tropospheric westerly anomalies associated with the stratospheric year-to-year variability is similar to the westerly (and SAM) response to the stratospheric ozone depletion (Figure S3a) in this season (Figure S6a). The similarity is consistent with previous studies [*Thompson et al.*, 2011; *Sun et al.*, 2014]. In contrast, the tropospheric westerly signal associated with the stratospheric year-to-year variability is not reproduced in the experiments without the oceanic front (Figures 3d and S6b); they also fail to reproduce the westerly response to the ozone depletion (Figures 3b and S3b). The results are qualitatively the same if the reference date for the stratospheric variability to shifted to 1st November (Figures S7a-b). If the reference date is shifted to 1st December, however, significant tropospheric anomalies emerge even without the oceanic front (Figure S7d). Still, their amplitude is considerably smaller, reaching only half of that in the experiments with the oceanic front (Figure S7c). In fact, the early-summer tropospheric SAM variability is significantly coupled with the late-spring stratospheric variability only in the presence of the oceanic front

(Figure S8).

The striking difference in the vertical SAM coupling in our experiments can be understood from a viewpoint of the troposphere SAM signature (Figure S2f). As discussed in previous studies [*Nakamura et al.*, 2008; *Sampe et al.*, 2013], the SST front strengthens the climatological mean eddy-driven westerlies in subpolar and mid-latitudes throughout the depth of the troposphere (Figure S2c) by activating synoptic-scale eddies (Figures S2d-e). Manifested as the variability of the eddy-driven jet, the SAM cannot be simulated realistically without the oceanic front (Figure S2f) nor the triggering effect of SAM on the downward coupling of the unforced internal variability of the stratospheric polar vortex into the troposphere. Indeed, the tropospheric SAM anomaly in summer is strongly coupled with the stratospheric variability only in the presence of oceanic front (Figure S6c-d). The distinct similarity in the structure of the westerly anomalies associated with the stratospheric/tropospheric dominant mode of variability (Figures S6a and S6c) indicates the importance of SAM representation in the troposphere for the vertical coupling. Furthermore, the observed distinct maximum in the persistence of a given phase of the early-summer tropospheric SAM when linked to the stratospheric variability (Figure 1B of *Baldwin et al.,* 2003; see supporting information for details) is simulated in the presence of the SST front (Figure S10a), while the persistence is considerably shorter in the absence of the front (Figure S10b). The realistic representation of the tropospheric SAM with the SST front can also enhance the persistence of the tropospheric westerly anomalies (Figure 3c), leading to the reproduction of the ozone-induced westerly response (Figure 3a).

5. Impact of SST front on the ozone-induced climatic trend found in CMIP3/5 models

We also find in more sophisticated global climate models that the ozone-induced trend in the lower-tropospheric westerlies in the summertime extratropical SH can be influenced by the representation of the midlatitude oceanic front. We analyze outputs of multiple climate models that participate in the Phases 3 and 5 of Coupled Model Intercomparison Project (CMIP3 [*Meehl et al.*, 2007] and CMIP5 [*Taylor et al.*, 2012], respectively) (See supporting information for details). It has already been shown that some of the CMIP3 models with realistic stratospheric ozone forcing can reproduce the SH climate changes [*Cai and Cowan,* 2007; *Son et al.*, 2009], and that those CMIP3 models with ozone recovering tend to project different climate changes than those without it [*Son et al.*, 2008]. A scatter plot in Figure 4 shows relationship between the climatological latitudes of oceanic fronts and the peak latitudes of the enhancing trends in 850-hPa zonal-mean westerlies both in austral summer simulated in the 23 CMIP3 models and 50 CMIP5 models listed in Tables S1 and S2, respectively. Those two latitudes indicate no obvious inter-model correlation if all the 73 models are considered. However, the correlation greatly increases up to +0.51 with significance exceeding the 10% level, if computed for the 12 models each of which simulates cross-frontal SST gradient stronger than the climatological SST gradient in the JRA-25 reanalysis data [*Onogi et al.*, 2007] and a significant cooling trend (at the 1% level) in the Antarctic stratosphere during the last 20 years of the 20th century (red circles in Figure 4). The temperature trend was evaluated at the 100-hPa level as a horizontal average poleward of 70°S in spring through early summer (October-January). The corresponding stratospheric cooling trend in the JRA-25 reanalysis is significant at the same level (1%). This significant positive correlation is consistent with our AGCM experiments; a strong midlatitude oceanic front acts to anchor the storm track and associated eddy-driven PFJ in a climate model, determining the nodal latitude of SAM and thereby the latitude of the ozone-induced westerly acceleration. In contrast, the inter-model correlation (+0.25) between these two latitudes loses its significance for the 21 models (blue triangles in Figure 4) that simulate significant cooling trends in the Antarctic stratosphere, but weaker midlatitude SST gradients than in the reanalysis. Figure 4 also indicates that westerly acceleration cannot be simulated realistically in the majority of the 15 models (marked with yellow circles in Figure 4) in which the midlatitude SST gradients are stronger than in the reanalysis but the stratospheric cooling is insignificant.

It is noteworthy that the relationship between the peak latitude of the westerly trend and frontal latitude in the JRA-25 reanalysis is very close to that derived from the linear regression (red line in Figure 4) among the 12 models that simulate strong oceanic fronts and significant stratospheric cooling trend. In contrast, deviations from that linear relationship tend to be greater for those models with weaker oceanic fronts even if the stratospheric cooling trend is significantly strong (blue triangles in Figure 4). These statistics suggest that an oceanic front, if it has enough intensity, may control the latitude of the maximum westerly acceleration in response to the stratospheric trend, presumably through enhanced eddy activity and eddy-driven jet. The statistics also suggest that realistic representation of the oceanic front is crucial for reliable future projection of the SH climate in a climate model under the forcing of the expected ozone recovery [*Thompson et al.,* 2011; *Son et al.,* 2008] and further global warming [*Shindell and Schmidt*, 2004; *Cai and Cowan*, 2007]. Note that no significant relationship can be found between the mean oceanic front intensities and 20-year trends in the westerly jet intensity or latitude (not shown). In other words, a stronger oceanic front, if simulated in a particular model, does not necessarily lead to a stronger trend in the westerly jet. This may be because the westerly trend in the complex CMIP models can be influenced by many other factors than the oceanic front intensity. For example, the stratospheric ozone depletion and other forcings are represented differently among the models (we used both CMIP3 and 5 to enhance the statistical confidence). The model top altitude can also influence the westerly jet latitude and its trend in the Southern Hemisphere [*Wilcox et al.,* 2012]. Different representation of tropical SST among the models may have also influenced the trend in the extra-tropics. However, the impact of the SST front includes not only its strength but also its latitudinal position. In fact, the latitudinal position of SST front in our experiments is also an important characteristic of the observed SST. The activity of baroclinic eddies and the eddy-driven westerlies are found to be sensitive to both its strength and its latitudinal shift (Nakamura et al., 2008; Ogawa et al., 2012). Figure 4 suggests that the latitudinal position of SST front can also impact on the internal tropospheric dynamics driving the observed stratosphere/troposphere coupling. In our analysis on CMIP models, the dynamical tropospheric changes associated with the latitudinal shift of the SST front was more detectable than the dynamical changes due to the strength of SST front.

6. Summary and discussion

The present study reveals the particular importance of a midlatitude oceanic front for the ozone-induced downward stratosphere/troposphere coupling and resulting tropospheric SAM-response. Our idealized aqua-planet AGCM experiments with prescribed zonally symmetric SST profile shows that the ozone-induced response as the tropospheric SAM occur only in the presence of SST front through enhanced vertical coupling of SAM as observed. Our results support the role of synoptic and planetary-scale waves in the mechanisms proposed for the downward stratosphere/troposphere coupling [*Yang et al.,* 2015]. One may wonder how significantly the slight overestimation of the subtropical jet intensity in our model (Figures S2a-b) can affect the SAM response, which is left for our future study. We nevertheless stress that the realistic representation of midlatitude eddy-driven jet in the presence of oceanic front is important for the tropospheric SAM response to the ozone depletion. Our analysis on the CMIP3/5 models suggests that the representation of a strong oceanic front in a model is important to reproduce the ozone-induced tropospheric SAM trend as observed. It should be noted that a strengthening of the SST front driven by the ozone-induced SAM trend [*Sen Gupta and England*, 2006, 2007] is indeed hinted in some of those models (Figure S11a), but not all of models with "stronger" SST fronts simulate positive trends in the front intensity (Figure S11b). Since the trend of SST front intensity is very weak (at most ~0.05 K/latitude per 20 years) compared to its climatological strength, the trend is unlikely to affect the selection of "stronger" and "weaker" SST fronts in our analysis. It is nevertheless suggested that an accurate simulation of oceanic front is important in projecting southern hemispheric ozone-induced climate change.

Acknowledgments

We used the ECHAM5 in support of Max-Plank Institute (MPI), Deutsches Klimarechenzentrum (DKRZ), and the Norddeutscher Verbund für Hoch—und Höchstleistungsrechnen. We thank Benjamin Moebis for his advices for our experiments. This collaborative work was initiated under the Germany-Japan Bilateral Joint Research Project funded by the Japan Society for the Promotion of Science (JSPS) and Deutsche

Forschungsgemeinschaft (DFG) (Co-PIs: S. Minobe and N. Keenlyside). This study is supported in part by the Japanese Ministry of Environment through the Environment Research and Technology Development Fund A-1201 and 2-1503 and by the Japanese Ministry of Education, Culture, Sports, Science and Technology (MEXT) through a Grant-in-Aid for Scientific Research in Innovative Areas 2205. We acknowledge the World Climate Research Program's Working Group on Coupled Modeling, which is responsible for CMIP, and we thank all contributing climate modeling groups listed in Tables S1 and S2. The U.S. Department of Energy's Program for Climate Model Diagnosis and Intercomparison provided coordination and support for CMIP, and led the development of software infrastructure in partnership with the Global Organization for Earth System Science Portals. We also acknowledge the "Data Integration and Analysis System" Fund (DIAS) for National Key Technology and the Innovative Program of Climate Change Projection for the 21st Century ("Kakushin" program) from MEXT. We thank Professor Matthew England and two anonymous reviewers for their valuable comments.

References

Andrews D. G., J. R. Holton, and C. B. Leovy, 1987: *Middle Atmosphere Dynamics.* Academic Press, San Diego.

Baldwin, M. P., D. B. Stephenson, D. W. J. Thompson, T. J. Dunkerton, A. J. Charlton, and A. O' Neill (2003), Stratospheric memory and skill of extended-range weather forecasts, *Science*, *301*, 636–640, doi:10.1126/ science.1087143.

Cai, W., and T. Cowan (2007), Trends in Southern Hemisphere circulation in IPCC AR4 models over 1950–99: Ozone depletion versus greenhouse forcing, *J. Clim., 20*, 681–693, doi:

10.1175/JCLI4028.1.

Gillett, N. P., and D. W. J. Thompson (2003), Simulation of recent Southern Hemisphere climate change, *Science, 302*, 273–275, doi: 10.1126/science.1087440.

Hotta, D., and H. Nakamura (2011), On the significance of sensible heat supply from the ocean in the maintenance of mean baroclinicity along storm tracks, *J. Clim., 24*, 3377–3401, doi: 10.1175/2010JCLI3910.1.

Limpasuvan, V., and D. L. Hartmann (2000), Wave-maintained annular modes of climate variability, *J. Clim., 13,* 4414–4429.

Lorenz, D. J., and D. L. Hartmann (2001), Eddy-zonal flow feedback in the Southern Hemisphere, *J. Atmos. Sci., 58*, 3312–3327.

Marshall, G. J. (2003), Trends in the Southern Annular Mode from observations and reanalyses, *J. Clim., 16*, 4134–4143.

Meehl G. A. *et al.* (2007), The WCRP CMIP3 multi-model dataset: A new era in climate change research, *Bull. Am. Meteorol. Soc., 88*, 1383–1394, doi: 10.1175/BAMS-88-9-1383.

Nakamura, H., T. Sampe, Y. Tanimoto, and A. Shimpo (2004), Observed associations among storm tracks, jet streams and midlatitude oceanic fronts, *AGU Geophys. Monogr., 147*, 329–345, doi: 10.1029/147GM18.

Nakamura, H., T. Sampe, A. Goto, W. Ohfuchi, and S.-P. Xie (2008), On the importance of midlatitude oceanic frontal zones for the mean state and dominant variability in the tropospheric circulation, *Geophys. Res. Lett., 35*, L15709, doi: 10.1029/2008GL034010.

Nonaka, M., *et al.* (2009), Air-sea heat exchanges characteristic of a prominent midlatitude oceanic front in the South Indian Ocean as simulated in a high-resolution coupled GCM, *J.*

Clim., 22, 6515–6535, doi: 10.1175/2009JCLI2960.1.

Ogawa, F., H. Nakamura, K. Nishii, T. Miyasaka, and A. Kuwano-Yoshida (2012), Dependence of the climatological axial latitudes of the tropospheric westerlies and storm tracks on the latitude of an extratropical oceanic front, *Geophys. Res. Lett., 39*, L05804, doi: 10.1029/2011GL049922.

Onogi, K. *et al.* (2007), The JRA-25 reanalysis, *J. Meteorol. Soc. Jpn., 85*, 369–432, doi: 10.2151/jmsj.85.369.

Polvani, L. M., D. W. Waugh, G. J. P. Correa, and S.-W. Son (2011), Stratospheric ozone depletion: The main driver of twentieth-century atmospheric circulation changes in the Southern Hemisphere, *J. Clim., 24*, 795–812, doi: 10.1175/2010JCLI3772.1.

Reynolds, R. W. *et al.* (2007), Daily high-resolution-blended analyses for sea surface temperature. *J. Clim., 20*, 5473–5496, doi: 10.1175/2007JCLI1824.1.

Roeckner, E. *et al.* (2003), The atmospheric general circulation model ECHAM5. Part I: Model description. *Max Planck Institute for Meteorology Rep., 349*, 127 pp.

Sampe, T., H. Nakamura, and A. Goto (2013), Potential influence of a midlatitude oceanic frontal zone on the annular variability in the extratropical atmosphere as revealed by aqua-planet experiments, *J. Meteorol. Soc. Jpn., 91a*, 243–267, doi: 10.2151/jmsj.2013-A09.

Scinocca, J. F., and P. H. Haynes (1998), Dynamical forcing of stratospheric planetary waves by tropospheric baroclinic eddies, *J. Atmos. Sci., 55*, 2361–2392.

Sen Gupta, A., and M. H. England (2006), Coupled ocean–atmosphere–ice response to variations in the Southern Annular Mode, *J. Clim.*, *19*, 4457–4486, doi: 10.1175/JCLI3843.1.

Sen Gupta, A., and M. H. England (2007), Coupled ocean–atmosphere feedback in the Southern Annular Mode, *J. Clim.*, *20*, 3677-3692, doi: 10.1175/JCLI4200.1.

Shindell, D., and G. A. Schmidt (2004), Southern Hemisphere climate response to ozone changes and greenhouse gas increases, *Geophys. Res. Lett., 31,* L18209, doi: 10.1029/2004GL020724.

Son, S.-W. *et al.* (2008), The impact of stratospheric ozone recovery on the Southern Hemisphere westerly jet, *Science, 320*, 1486–1489, doi: 10.1126/science.1155939.

Son, S.-W., N. F. Tandon, L. M. Polvani, and D. W. Waugh (2009), Ozone hole and Southern Hemisphere climate change, *Geophys. Res. Lett., 36*, L15705, doi: 10.1175/JCLI-d-13-00698.

Sun, L., G. Chen, and W. A. Robinson (2014), The role of stratospheric polar vortex breakdown in Southern Hemisphere climate trends, *J. Atmos. Sci., 71*, 2335–2353, doi: 10.1175/JAS-d-13-0290.1.

Taylor, K. E., R. J. Stouffer, and G. A. Meehl (2012), An overview of CMIP5 and the experiment design, *Bull. Am. Meteorol. Soc., 93*, 485–498, doi: 10.1175/BAMS-d-11-00094.1.

Thompson, D. W. J., and J. M. Wallace (2000), Annular modes in the extratropical circulation. Part I: Month-to-month variability, *J. Clim., 13*, 1000–1016.

Thompson, D. W. J., and S. Solomon (2002), Interpretation of recent Southern Hemisphere climate change, *Science, 296*, 895–899, doi: 10.1126/science.1069270.

Thompson, D. W. J., M. P. Baldwin, and S. Solomon (2005), Stratosphere–troposphere coupling in the Southern Hemisphere, *J. Atmos. Sci., 62*, 708–715, doi: 10.1175/JAS-3321.1.

Thompson D. W. J. *et al.* (2011), Signatures of the Antarctic ozone hole in Southern Hemisphere surface climate change, *Nature Geoscience, 4*, 741–749, doi: 10.1038/ngeo1296.

Wilcox, L. J., A. J. Charlton-Perez, and L. J. Gray (2012), Trends in austral jet position in ensembles of high- and low-top CMIP5 models, *J. Geophys. Res., 117,* D13115, doi:10.1029/2012JD017597.

Yang, H., L. Sun, and G. Chen (2015), Separating the mechanisms of transient responses to stratospheric ozone depletion-like cooling in an idealized atmospheric model, *J. Atmos. Sci., 72*, 763–773, doi:10.1175/JAS-D-13-0353.1.

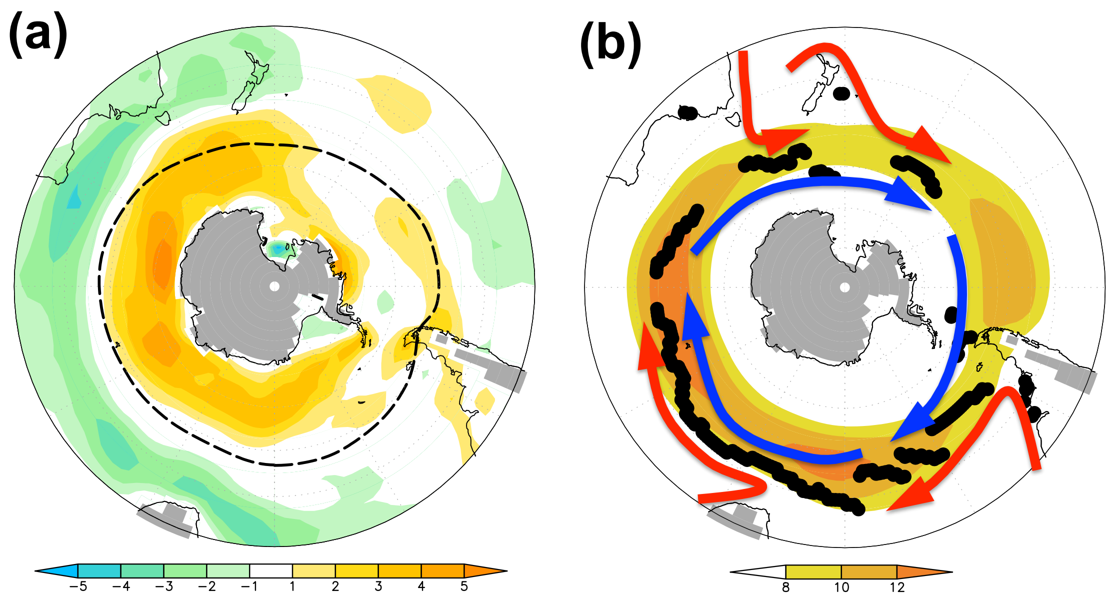

Figure 1. Trend in near-surface westerlies over the midlatitude SH observed during the last 21 years of the 20th century (1979/80-2000/01), and climatological axes of the westerlies and oceanic front. The (a) linear trend (m s^{-1}/21years; contour) and (b) climatology of December-January mean 925-hPa zonal wind (m s^{-1}; shade). The dashed line in (a) indicates the axial latitude of the climatological westerlies. Superimposed on (b) are climatological axis of the midlatitude oceanic front (black dots; marked as the peak latitude of meridional SST gradient) and major warm and cool ocean currents (red and blue arrows, respectively). Gray shades indicate the absence of the 925hPa pressure level due to topography.

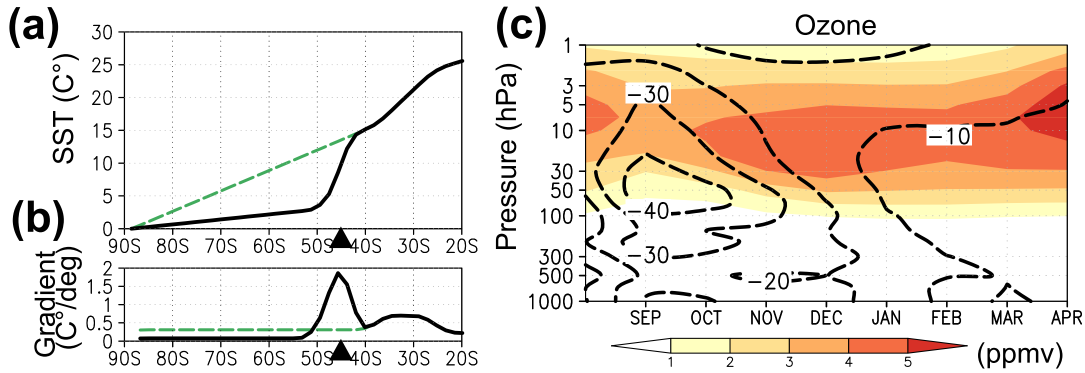

Figure 2. SST and ozone profiles prescribed in AGCM experiments. (a)-(b) latitudinal profiles of (a) SST and (b) its meridional gradient averaged from 1st November to 31st December for the experiments with (black) and without (green) the oceanic front. (c) height-time section of the zonally-uniform ozone concentration (ppmv; shade) averaged over the polar latitudes (75~90°S) for the low-ozone period and its fractional depletion (%) from the high-ozone period (dashed lines).

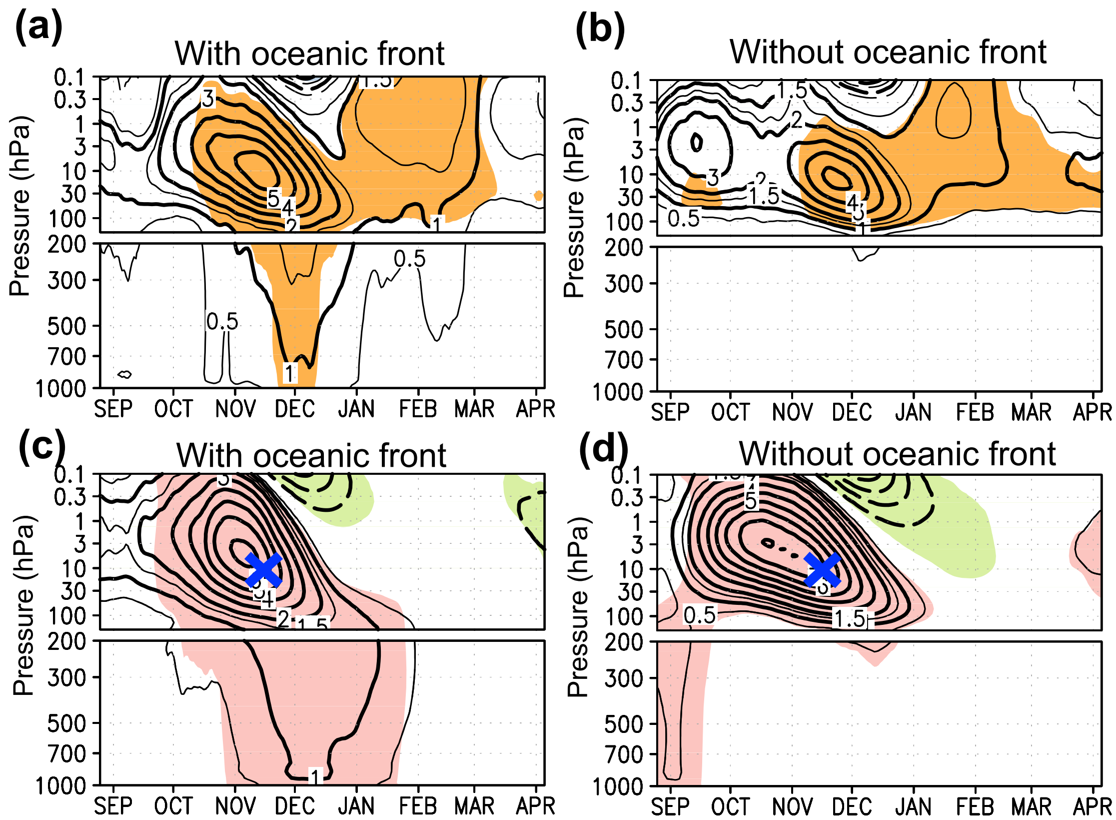

Figure 3. Time-height sections showing the seasonality of the simulated 31-day running-mean westerly response to the prescribed ozone depletion and anomalous westerlies associated with the stratospheric internal variability. (a)-(b) zonal-mean westerly response (m s^{-1}; contour) averaged between 45°S and 60°S for experiments (a) with and (b) without the oceanic front. Shading indicates the 5% statistical significance based on the Student's *t*-test. (c)-(d) Typical 31-day running-mean anomalies in zonal-mean zonal wind (m s^{-1}) associated with year-to-year variability, regressed linearly on its PC1 time series at 13hPa (see text for details) in experiments (c) with the oceanic front and (d) without it. The reference pressure level (13hPa) and reference date (15th November) for the EOF analysis are marked by a cross in each panel. Shading indicates statistically significant signal at the 5% level estimated from the correlation coefficient.

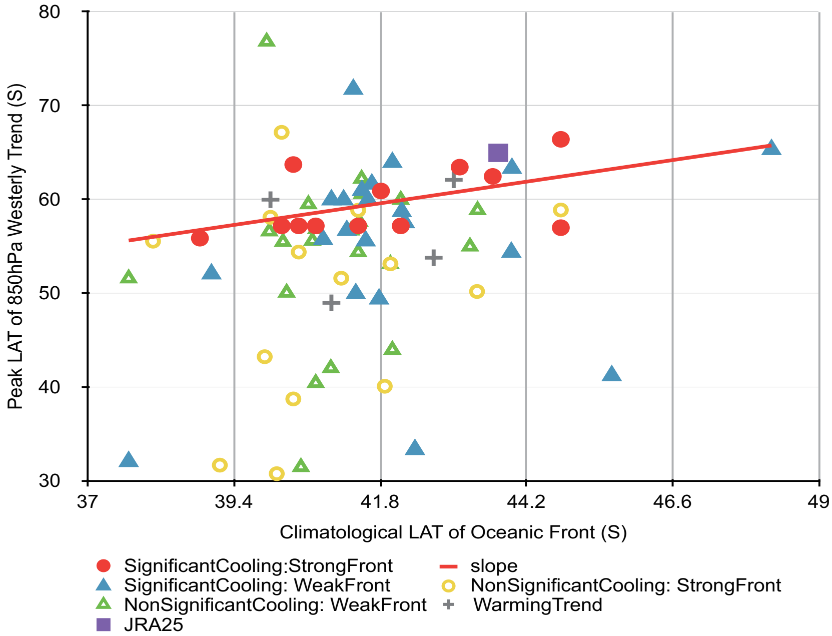

Figure 4. A scatter plot for the CMIP3/5 global climate models showing the relationship between summertime (Dec-Feb) climatological latitude of the midlatitude oceanic front (abscissa) and the peak latitude of an increasing trend in 850-hPa summertime zonal-mean westerlies (ordinate). The linear trend is evaluated at each latitudinal grid point for the period 1979/80-1998/99. A purple square indicates those latitudes in the JRA25 data based on observations. Red line represents a linear regression among the 12 models (marked with red circles) that simulate midlatitude oceanic fronts stronger than in the JRA-25 data and stratospheric cooling trends over Antarctica significant at the 1% level in spring and summer (Oct-Jan). Blue triangles signify those models in which the simulated stratospheric cooling trends are significant and midlatitude oceanic fronts are weaker than in JRA-25. Yellow circles signify those models in which the simulated stratospheric cooling trends are not significant and midlatitude oceanic fronts are stronger than in JRA-25. Green triangles signify those models in which the simulated stratospheric cooling trends are not significant and midlatitude oceanic fronts are weaker than in JRA-25. Black crosses signify four models that simulate warming trends in the Antarctic stratosphere rather than cooling.